Title

Senescence Increases Choroidal Endothelial Stiffness and Susceptibility to Complement Injury: Implications for Choriocapillaris Loss in AMD.

Journal

Investigative ophthalmology & visual science, 57(14)

ISSN

0146-0404

Authors

Cabrera, Andrea P
Bhaskaran, Arun
Xu, Jun
et al.

Publication Date

2016-11-01

DOI

10.1167/iovs.16-19727

Peer reviewed

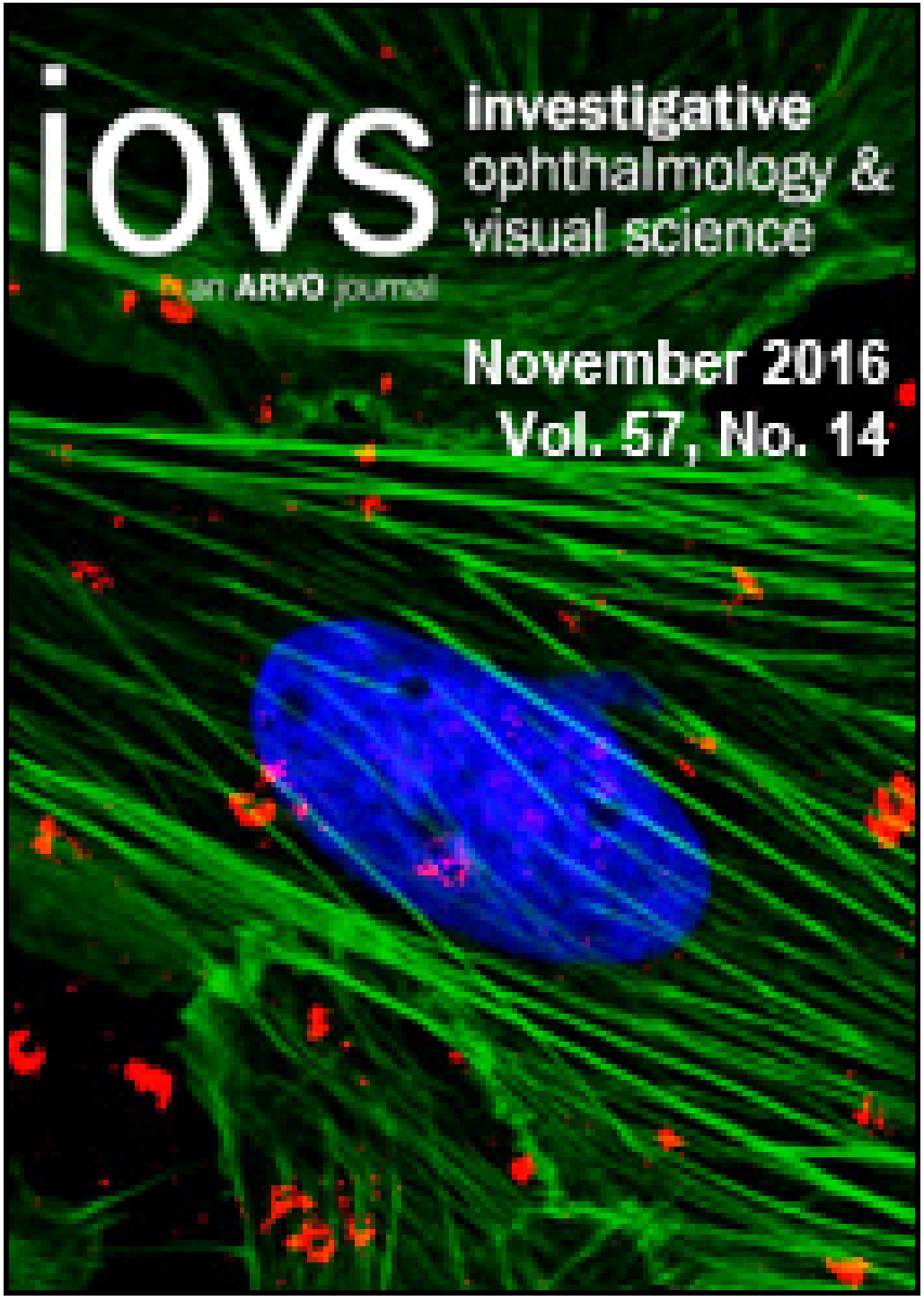
iovs
investigative
ophthalmology &
visual science
an ARVO journal
November 2016
Vol. 57, No. 14

Senescence Increases Choroidal Endothelial Stiffness and Susceptibility to Complement Injury: Implications for Choriocapillaris Loss in AMD

Andrea P. Cabrera,[1] Arun Bhaskaran,[1] Jun Xu,[2] Xiao Yang,[1] Harry A. Scott,[1] Umar Mohideen,[2] and Kaustabh Ghosh[1]

[1]Department of Bioengineering, University of California, Riverside, California, United States
[2]Department of Physics and Astronomy, University of California, Riverside, California, United States

Correspondence: Kaustabh Ghosh, Department of Bioengineering, University of California, Riverside, Riverside, CA 92521, USA; kghosh@engr.ucr.edu.

Submitted: April 11, 2016
Accepted: August 30, 2016

Citation: Cabrera AP, Bhaskaran A, Xu J, et al. Senescence increases choroidal endothelial stiffness and susceptibility to complement injury: implications for choriocapillaris loss in AMD. *Invest Ophthalmol Vis Sci*. 2016;57:5910–5918. DOI:10.1167/iovs.16-19727

Purpose. Age-related macular degeneration (AMD) commonly causes blindness in the elderly. Yet, it is untreatable in the large fraction of all AMD patients that develop the early dry form. Dry AMD is marked by the deposition of membrane attack complex (MAC) on choriocapillaris (CC), which is implicated in CC degeneration and subsequent atrophy of overlying retinal pigment epithelium. Since MAC is also found on the CC of young eyes, here we investigated whether and how aging increases choroidal endothelial susceptibility to MAC injury.

Methods. Monkey chorioretinal endothelial cells (ECs, RF/6A) were cultured to high passages (>P60) to achieve replicative senescence. We treated ECs with complement-competent human serum to promote MAC deposition and injury, which were assessed by flow cytometry and trypan blue exclusion assay, respectively. Stiffness of EC was measured by atomic force microscopy indentation while Rho GTPase activity was quantified by Rho G-LISA assay.

Results. Our findings reveal that senescent ECs are significantly stiffer than their normal counterparts, which correlates with higher cytoskeletal Rho activity in these cells and their greater susceptibility to complement (MAC) injury. Importantly, inhibition of Rho activity in senescent ECs significantly reduced cell stiffness and MAC-induced lysis.

Conclusions. By revealing an important role of senescence-associated choroidal EC stiffening in complement injury, these findings implicate CC stiffening as an important determinant of age-related CC atrophy seen in dry AMD. Future studies are needed to validate these findings in appropriate animal models so new therapeutic targets can be identified for treatment of dry AMD.

Keywords: aging, Rho, membrane attack complex, cell lysis, vessels

Age-related macular degeneration (AMD), a progressive disease affecting approximately 10 million in the US, is a leading cause of blindness in the aging population.[1,2] It manifests in two forms: the early-stage "dry" AMD that is clinically characterized by retinal pigment epithelium (RPE) atrophy and drusen accumulation between the RPE and underlying choriocapillaris (CC), and the late-stage "wet" AMD marked by abnormal choroidal neovascularization and leakiness.[3] Current therapies approved by the US Food and Drug Administration only target 10% to 15% of all AMD patients who develop the vision-threatening wet stage[3,4] while no therapies exist for the more prevalent dry form. Since dry AMD is a potential risk factor for late-stage wet AMD, there is a recognition that more effective AMD management can be achieved by tackling the disease at the early stage.

Dry AMD is characterized by significant CC degeneration.[5,6] Since the CC is essential for maintenance of RPE homeostasis and viability, CC dropout and associated loss of perfusion have been implicated in RPE hypoxia and atrophy.[3,7,8] This potential role of CC degeneration in the pathogenesis of dry AMD necessitates identification of the factors that contribute to the loss of CC in this condition.

Past studies have revealed that dry AMD is marked by complement activation in the sub-RPE space,[9,10] which leads to the deposition of membrane attack complex (MAC; C5b-9) on the CC.[5,11] Since MAC forms pores in cell membrane and causes cell lysis, it may contribute to choroidal endothelial loss and CC degeneration associated with dry AMD. Indeed, the degenerating CC in old eyes with dry AMD exhibit strong MAC deposition,[11] which is consistent with the hypothesis of MAC-induced CC degeneration. Interestingly, MAC is also abundant on the healthy CC of young eyes.[11] Thus, it is likely that specific age-related factors exacerbate the putative degenerative effects of MAC on the CC.

One potential age-related factor is vascular stiffness. Past studies have shown that aging is associated with stiffening of retinal vessels and the sclera,[12,13] while separate studies in nonophthalmic vessels such as aorta and arteries have indicated that age-related vascular stiffening enhances vascular sensitivity to proinflammatory cues.[14–16] Such aberrant stiffness-dependent vascular dysfunction results from altered endothelial

Investigative Ophthalmology & Visual Science

cytoskeletal tension (contractility) and mechanotransduction, the process by which mechanical cues get transduced into intracellular biochemical signaling pathways.[17–23] However, whether aging is associated with increased cytoskeleton-mediated choroidal endothelial stiffening and enhanced CC sensitivity to MAC remains unknown.

Using choroidal endothelial senescence as an in vitro model of CC aging, we here show that senescence leads to a significant increase in endothelial cell (EC) stiffness, which correlates with increased complement injury. Notably, the increased stiffness of senescent ECs correlated with greater Rho activity, which is associated with cell tension and stiffness. Finally, we demonstrate that pharmacological modulation of Rho-dependent EC stiffness alone reverses the degenerative effects of complement activation on ECs.

Materials and Methods

EC Culture

Monkey chorioretinal ECs (RF/6A) were purchased from ATCC (Manassas, VA, USA) and grown in Eagle's minimum essential medium (EMEM, ATCC) supplemented with 10% fetal bovine serum (FBS; Thermo Fisher Scientific, Inc., Waltham, MA, USA) and 1x antibiotic-antimycotic mixture (Thermo Fisher Scientific, Inc.). The RF/6A EC culture was maintained at 37°C in a humidified atmosphere with 5% CO_2, with culture medium being replaced every 2 days. For all in vitro studies, culture dishes were coated with 0.1% gelatin (Sigma Aldrich Corp., St Louis, MO, USA) to facilitate robust RF/6A EC adhesion and spreading during the assays.

Detection of EC Senescence

To achieve replicative senescence, lower passage RF/6A ECs were serially expanded by splitting at a 1:3 ratio every 3 days for $\geq$20 passages. To confirm replicative senescence, low and high passage RF/6A ECs were subjected to X-gal staining, which detects expression of β-galactosidase (β-Gal), a reliable cell senescence marker.[24,25] Specifically, cells were plated at a low density (20,000 cells/cm^2) in starvation medium (EMEM containing 0.5% FBS) for 6 hours. Next, ECs were rinsed twice with ice-cold PBS and fixed with 0.25% glutaraldehyde (Electron Microscopy Sciences, Hatfield, PA, USA) at room temperature (RT) for 10 minutes with gentle rocking. Fixed RF/6A ECs were rinsed twice with ice-cold PBS and incubated in freshly prepared staining solution containing 1 mg/mL X-Gal (Thermo Fisher Scientific, Inc.), 5 mM potassium ferricyanide (Sigma-Aldrich Corp.), 5 mM potassium ferrocyanide (Sigma-Aldrich Corp.), and 2 mM $MgCl_2$ (Sigma-Aldrich Corp.) for 6 hours at 37 °C. Brightfield images of stained cells ($n = 18$ per condition) were acquired using a microscope (Nikon Eclipse Ti; Nikon Corp., Tokyo, Japan) fitted with a camera (Nikon Digital Sight DS-Fi1U2; Nikon Corp.) and, following intensity thresholding, the percentage of cells stained by X-gal was quantified using ImageJ (http://imagej.nih.gov/ij/; provided in the public domain by the National Institutes of Health, Bethesda, MD, USA).

Quantitative RT-PCR

Total RNA was isolated from RF/6A EC monolayers (three replicates/condition) using an RNA purification kit (Direct-zol RNA MiniPrep; Zymo Research, Irvine, CA, USA), converted to cDNA with high capacity cDNA reverse transcription (Thermo Fisher Scientific, Inc.), and amplified with the appropriate TaqMan assay for p21 or CD31 primers (Thermo Fisher Scientific, Inc.) on the CFX connect real-time PCR detection system (BioRad, Hercules, CA, USA). Relative mRNA levels were determined by the comparative cycle threshold method with normalization to glyceraldehyde 3-phosphate dehydrogenase (GAPDH; Thermo Fisher Scientific, Inc.).

Complement Activation

To examine the effects of complement activation on RF/6A ECs, cells were plated in starvation medium for 6 hours prior to replacement of medium with veronal buffered saline (VBS; composed of NaCl 145 mM, sodium barbital 1.8 mM, barbituric acid 3 mM, $CaCl_2$ 50 μM and 250 μM $MgCl_2$, adjusted to pH 7.4) containing 10% normal human serum (NHS; Complement Technology, Inc., Tyler, TX, USA) for 2 hours at 37°C to promote complement activation. Monkey chorioretinal ECs that were NHS-treated were then either detached for flow cytometry analysis of surface MAC deposition or subjected to trypan blue exclusion assay for determination of cell lysis. To pharmacologically inhibit the senescence-associated effects of cell stiffness, cells were incubated with 1, 2.5, or 5 μM of Y27632 (Rho/ Rho-associated kinase [ROCK] inhibitor; Sigma-Aldrich Corp.) in VBS containing 10% NHS for 2 hours at 37°C. To activate Rho/ROCK–dependent cell stiffness, cells were incubated with 0.025 or 0.05 U/mL Thrombin (Sigma) in VBS containing 10% NHS for 2 hours at 37°C.

Flow Cytometry

Monkey chorioretinal ECs were detached and labeled with PE-labeled mouse anti-human CD146 antibody (BD Biosciences, San Jose, CA, USA) or mouse anti-monkey CD59 antibody (AbCam, Cambridge, UK). Next, RF/6A ECs were fixed with 1% paraformaldehyde (PFA; Electron Microscopy Sciences), detected with a flow cytometer (Cell Lab Quanta SC Beckman Coulter, Brea, CA, USA), and analyzed by single cell analysis software (FlowJo; Treestar, Inc., Ashland, OR, USA). For deposition studies with MAC, RF/6A ECs treated with 10% NHS were detached and labeled with mouse anti-C5b-9 antibody (Abcam), followed by fluorescently labeled anti-mouse IgG (BD Biosciences).

Trypan Blue Exclusion Assay

The RF/6A ECs were plated at a low density in starvation medium for 6 hours before treatment with 10% NHS for 2 hours at 37°C, followed by the addition of 0.1% trypan blue (Thermo Fisher Scientific, Inc.) in PBS for 8 minutes at RT. Next, RF/6A ECs were rinsed twice with PBS twice and fixed with 1% PFA for 10 minutes. Brightfield images of stained cells ($n = 18$ per condition) were acquired using a microscope (Nikon Corp.) fitted with a Nikon Digital Sight DS-Fi1U2 camera (Nikon Corp.), and the percentage of cells stained by trypan blue was quantified using ImageJ.

Measurement of EC Stiffness

For measurement of EC stiffness, cells were grown to confluence on sterile 0.1% gelatin-coated cover slips. Next, the confluent EC monolayers were maintained overnight in starvation medium prior to indentation with a biological-grade atomic force microscope (AFM; Veeco Instruments, Plainview, NY, USA). Specifically, cell stiffness was measured in tapping mode using a 5-μm spherical glass bead attached to the silicon nitride tip of a 140-μm long microcantilever (MLCT, Bruker, Billerica, MA, USA) with bending spring constant of 0.1 N/m. Force curves were obtained and analyzed as per our established protocol.[22] In some measurements, senescent ECs were treated with Y27632 (5 μM; 2 hours at 37°C in

starvation media), a pharmacologic inhibitor of Rho/ROCK activity, prior to AFM force indentation.

Rho Activity

Confluent EC monolayers were lysed using RIPA lysis and extraction buffer (G-Biosciences, St. Louis, MO, USA) supplemented with protease and phosphatase inhibitor cocktails (Boston BioProducts, Ashland, MA, USA). RhoA activity was measured from cell lysates using the RhoA G-LISA activation assay kit (Cytoskeleton, Inc, Denver, CO, USA), per the manufacturer's protocol. Results were obtained by measuring absorbance at 490 nm using a plate reader (Victor2; Perkin Elmer, MA, USA).

Actin Cytoskeleton Staining

The RF/6A ECs were plated at a low density in regular culture medium for 24 hours prior to overnight culture in starvation medium. Next, the cells were fixed in 4% PFA for 15 minutes, rinsed with PBS, and permeabilized using 0.2% Triton X-100 (in 1 mg/mL BSA). To block nonspecific binding, cells were incubated in 2% (wt/vol) BSA for 30 minutes at RT. Next, a 1:200 dilution of AlexaFluor 594 Phalloidin (Thermo Fisher Scientific, Inc.) in 2% BSA was added to cells for 20 minutes in the dark at RT, followed by mounting of the cells on glass slides for fluorescence imaging. For visualization of actin stress fibers, phalloidin-labeled mounted EC cultures were imaged using Nikon Eclipse TI microscope fitted with a Nikon DS-Qi1Mc camera (Nikon Corp.). ImageJ was used to quantify the average number of actin stress fibers per cell from three separate regions along the long axis ($n \geq 20$ cells per condition).

Measurement of Cell Area

To quantify cell area, ECs were plated on plastic culture dishes for 24 hours before being subjected to phase contrast imaging using the aforementioned microscope (Nikon Corp.). Projected cell area ($n = 250$ cells/condition) was measured by tracing the cell perimeter using ImageJ.

Statistics

All data were obtained from multiple cells and multiple replicates/condition (as indicated in each respective section) and expressed as mean ± standard error or standard deviation, as indicated. Statistical significance was determined using analysis of variance (ANOVA), followed by Tukey's and Bonferroni post-hoc analysis (Instat; GraphPad Software Inc., La Jolla, CA, USA). Results were considered significant if $P < 0.05$.

Results

Senescence Increases Choroidal EC Susceptibility to Complement Injury

Cellular senescence recapitulates many features of aging.[25,26] Thus, to develop an in vitro model of CC aging, RF/6A ECs were cultured to high passages (>P60) to achieve replicative senescence and compared with lower passage (<P40) cells for expression levels of senescence-associated β-galactosidase (SA-β-gal), a well-known senescence marker.[24] Staining with X-gal, which yields a blue color when cleaved by SA-β-gal, revealed a 9-fold greater ($P < 0.001$) expression of SA-β-gal in higher passage cells than in the lower passage counterparts (Fig. 1A). To further confirm the senescent phenotype, we compared the expression levels of p21 in the low and high passage cells. p21 is an inhibitor of cyclin-dependent kinase that promotes cell growth arrest and, thereby, senescence.[27] Our qPCR measurements revealed that high passage ECs exhibit 1.7-fold higher levels ($P < 0.01$) of p21 mRNA than low passage ECs (Fig. 1B). Consistent with the typical senescence phenotype, we also observed a markedly greater percentage of "enlarged" cells (projected area >4000 μm^2) in the high passage ECs than in the lower passage cells (Supplementary Fig. S1). The low and high passage cells were subsequently termed "normal" and "senescent" ECs, respectively. Notably, the SA-β-gal–expressing senescent ECs did not exhibit any loss of endothelial phenotype, as judged by similar expression levels of classical endothelial-specific markers CD31 (Fig. 1C) and CD146 (Fig. 1D) in normal and senescent ECs.

To test their sensitivity to complement activation associated with dry AMD, we exposed these cells to complement-competent NHS. By activating the alternative complement pathway, NHS treatment leads to surface MAC deposition similar to that observed in the CC of human dry AMD eyes.[28,29] Flow cytometry analysis of NHS-treated normal and senescent ECs labeled with anti-C5b-9 (anti-MAC) revealed similar degrees of surface MAC deposition in these cells (Fig. 2A). However, when compared with normal ECs, the senescent cells underwent a 3-fold increase ($P < 0.001$) in complement-induced lysis, as judged by greater trypan blue incorporation within the senescent ECs (Fig. 2B, Supplementary Fig. S2). Notably, this increase in complement-induced lysis of senescent ECs did not result from reduced expression of endogenous cell-surface MAC inhibitory factor CD59, whose surface levels were comparable in both normal and senescent ECs (Supplementary Fig. S3). Predictably, the lysed (trypan blue-positive) cells exhibited a rounded morphology (Fig. 2B; inset), which is indicative of impaired cell viability and death.[30,31]

Senescence Is Associated With Increased Choroidal EC Stiffness

Past studies have shown that aging is associated with stiffening of aorta and arteries,[32,33] which also exhibit greater sensitivity to proinflammatory cues.[14,16] Thus, we asked whether the greater sensitivity of senescent RF/6A ECs to complement activation was caused, at least in part, by increased EC stiffness. Multiple force indentation measurements by a biological-grade AFM revealed that, indeed, senescent ECs are ~30% stiffer ($P < 0.01$) than normal ECs (Fig. 3).

Senescent Choroidal ECs Exhibit Higher Rho Activity

Rho is a key mechanotransduction player that regulates actin cytoskeletal tension and, as a consequence, cell stiffness.[19,34] Thus, we looked to see whether the increase in senescent EC stiffness results from a concomitant increase in Rho activity. Measurement of baseline Rho activity in confluent EC monolayers revealed that senescent ECs exhibit 1.4-fold higher ($P < 0.05$) Rho activity than normal ECs (Fig. 4A). Further, since Rho directly regulates actin cytoskeletal tension, its higher activity in senescent ECs predictably correlated with a 35% increase in actin stress fiber density in these cells (Fig. 4B).

Inhibition of Rho Activity Prevents Complement-Induced Lysis of Senescent ECs

To determine whether increased Rho-dependent cell tension (stiffness) exacerbates complement-induced lysis, we cotreated senescent ECs with NHS and a pharmacologic inhibitor

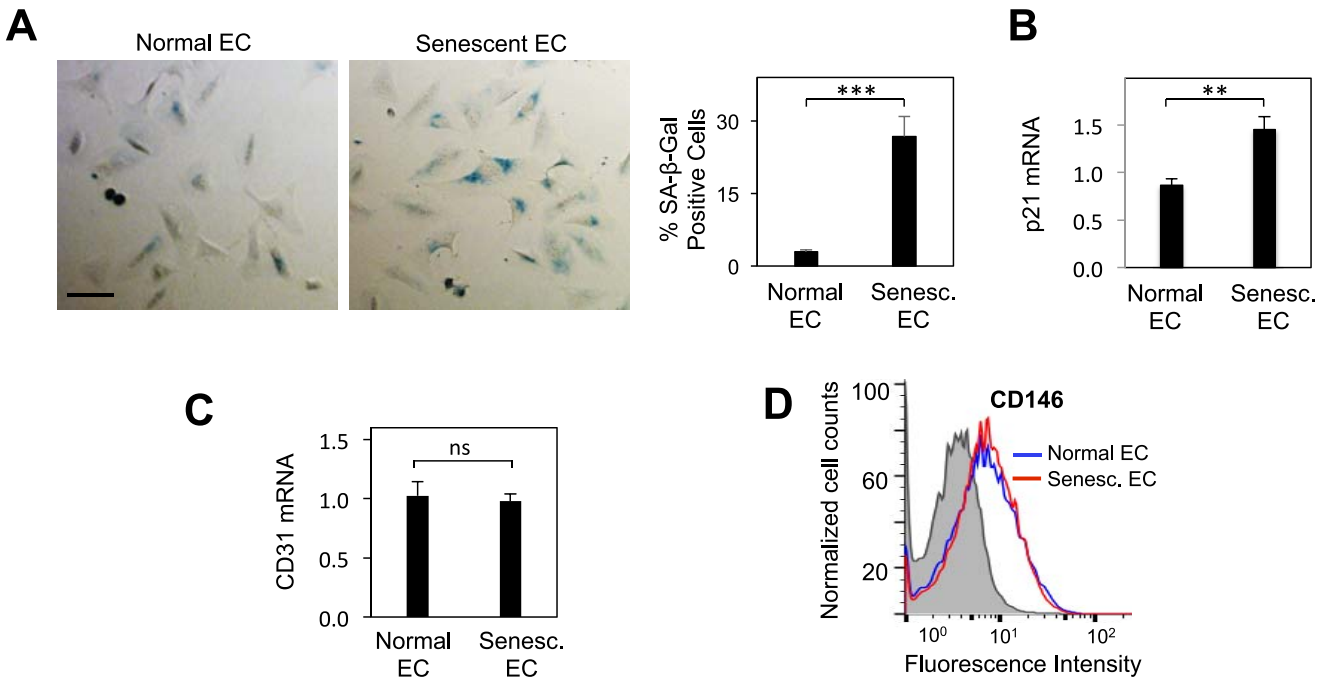

Figure 1. Senescent ECs exhibit high β-Gal expression. (**A**) Monkey chorioretinal ECs at low (<P40) and high (>P60) passages were subjected to X-gal staining, which stains β-gal (a senescence marker) blue. Representative brightfield images and net intensity measurements (*bar graph*) from multiple ($n > 1500$) cells reveal significantly greater β-gal expression in higher passage ("senescent") RF/6A ECs than in lower passage ("normal") cells. *** $P < 0.001$. *Bars* indicate average ± standard error of mean. *Scale bar*: 50 μm. (**B**) Quantitative RT-PCR analysis from multiple replicates ($n = 3$) shows that, when compared with low passage ECs, the high passage cells exhibit significantly higher p21 mRNA expression. ** $P < 0.01$. Levels of p21 mRNA were normalized with respect to GAPDH. *Bars* indicate average ± standard error of mean. (**C**) Quantitative RT-PCR analysis from multiple replicates ($n = 3$) shows that normal and senescent ECs exhibit similar levels of CD31 mRNA expression. Levels of CD31 mRNA were normalized with respect to GAPDH. *Bars* indicate average ± standard error of mean. (**D**) Normal and senescent ECs were labeled with anti-CD146 or isotype-matched control antibody (*solid gray histogram*), and subjected to flow cytometry. Histograms of cell counts versus fluorescence indicate that both normal and senescent cells exhibit similar expression levels of cell surface CD146. ns, no significance.

(Y27632) of ROCK, the immediate downstream target of Rho that controls myosin-dependent actin tension (cell stiffness). Our AFM measurements confirmed that Y27632 treatment causes a significant ($P < 0.05$) reduction in the stiffness of senescent ECs (Fig. 5A). More importantly, we found that inhibition of Rho/ROCK–dependent cell stiffness alone inhibits complement-induced cell lysis in a dose-dependent manner (IC_{50} ~2.5 μM; Fig. 5B), with the lysis observed at the highest Y27632 dose of 5 μM comparable with that seen in NHS-treated normal ECs.

Increasing Rho Activity in Normal ECs Exacerbates Complement Injury

To confirm the role of cell stiffness in complement injury, normal ECs were cotreated with NHS and thrombin, a Rho agonist that enhances actin cytoskeletal tension and cell stiffness.[35–37] As shown in Figure 6, thrombin treatment of normal ECs produced a dose-dependent increase ($P < 0.001$) in complement-induced cell lysis. That thrombin exacerbates complement injury by increasing Rho/ROCK–mediated cell

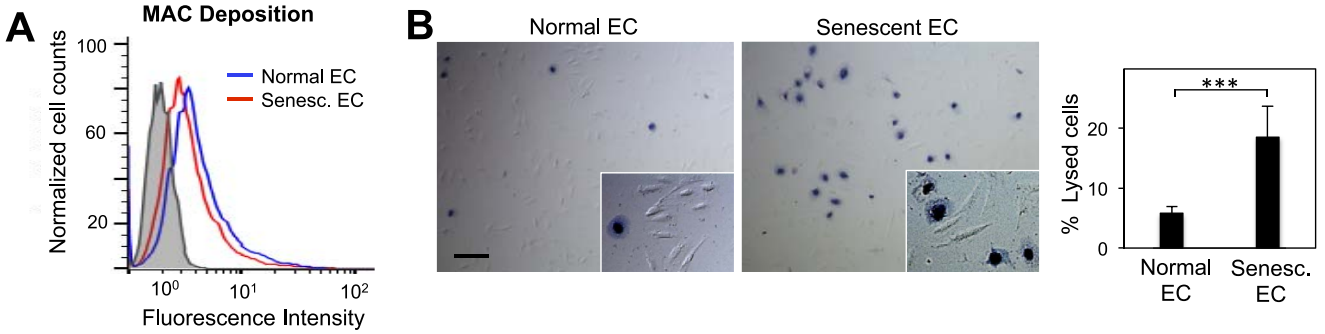

Figure 2. Senescence increases choroidal EC susceptibility to complement injury. (**A**) The RF/6A ECs were treated with complement-competent normal human serum (NHS, 10% vol/vol; 2 hours), labeled with anti-MAC (C5b-9) or isotype-matched control antibody (*solid gray histogram*), and subjected to flow cytometry to detect surface MAC deposition. Histograms of cell counts versus fluorescence indicate that both normal and senescent cells exhibit similar surface MAC deposition. (**B**) Lysis of NHS treated-cells was detected by trypan blue exclusion assay. Representative brightfield images and counting of trypan blue-loaded cells (*bar graph*; $n \geq 200$ cells) reveals significantly greater lysis of senescent RF/6A ECs than that of normal cells. *** $P < 0.001$. *Bars* indicate average ± standard deviation. *Scale bar*: 100 μm.

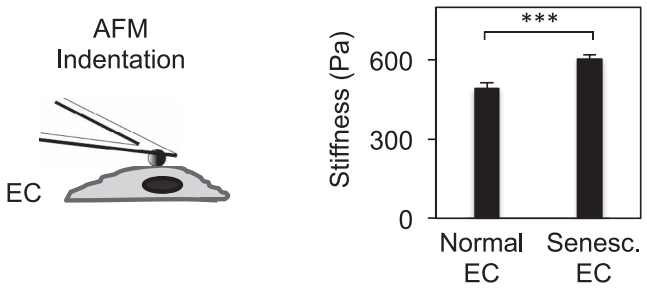

Figure 3. Senescent ECs exhibit increased stiffness. *Schematic*: EC stiffness was measured by indentation with a biological-grade AFM fitted with a silicon nitride cantilever tip containing a ~5 μm-diameter glass bead. *Bar graph*: Quantitative analysis of multiple ($n \geq 30$) force indentation measurements reveal a ~30% increase in the stiffness of senescent RF/6A ECs when compared with that of normal cells. *** $P < 0.001$. *Bars* indicate average ± standard error of mean.

tension (stiffness) and not via its ability to activate complement[38] was confirmed when cotreatment with Rho/ROCK inhibitor Y27632 prevented the increase in cell lysis by thrombin (Fig. 6).

Discussion

Although CC dropout is implicated in RPE atrophy associated with dry AMD, the precise mechanism(s) by which age-related CC degeneration occurs remains elusive. The observation that there is significant MAC deposition on the CC of old AMD eyes has led to the speculation that complement injury contributes to CC loss in dry AMD.[6,39,40] However, MAC is also found on the CC of young healthy eyes. Thus, here we tested the hypothesis that aging increases the susceptibility of choroidal ECs to MAC injury, thereby exacerbating EC lysis and CC degeneration. Using replicative senescence as an in vitro model of aging, we here show that senescent ECs exhibit greater MAC-induced lysis than their normal counterparts. Our studies further reveal that senescence leads to an increase in Rho-mediated cell stiffness that, in turn, contributes significantly to the increased susceptibility of senescent ECs to MAC injury. To our knowledge, this study is the first to identify a possible mechanism by which aging may contribute to CC loss associated with early AMD, thereby providing a rationale for performing detailed studies that examine Rho and EC stiffness as potentially new therapeutic targets for early AMD.

Aging is a major nonmodifiable risk factor for AMD. Yet, precisely how it contributes to AMD pathogenesis remains poorly understood. To study the effects of aging on the CC, we established an in vitro model of CC aging by culturing choroidal ECs to high passages, which leads to replicative senescence. Since cellular senescence is implicated in many age-related degenerative phenotypes,[25,41] we reasoned that senescent choroidal ECs will likely recapitulate the phenotype of aging CC in AMD eyes. We confirmed the induction of cellular senescence by staining for β-gal, measuring p21 mRNA expression and projected cell area, widely used phenotypic markers of cellular senescence. Conceptually, our observation that a cell line (RF/6A) deemed to be immortal exhibits markers of senescence at high passages appears paradoxical. However, in support of our observations, we would like to point out that RF/6A ECs have conventionally been used between passages 18 through 60[42–44] while the studies that used these higher passage cells never assessed the markers of senescence. Thus, to our knowledge, we are the first to use RF/6A ECs past the conventional passage number and measure expression of senescence markers. Consistent with our observations, nonendothelial cell lines transformed with SV40 have been demonstrated to exhibit lack of telomerase activity,[45] an independent marker of senescence.

Dry AMD is associated with subretinal inflammation, which is characterized by complement activation and inflammatory cell infiltration into the sub-RPE space. The infiltrating inflammatory cells are thought to further enhance complement activation either directly by undergoing activation[46,47] or indirectly by stimulating higher expression of complement factors by the RPE.[48] This subretinal inflammatory milieu leads to MAC deposition on the CC. Consistent with these observations, we show that treatment of choroidal ECs with complement-competent serum leads to surface MAC deposition. Intriguingly, however, we found that although MAC deposition was comparable on normal and senescent ECs, the latter underwent significantly greater MAC-induced lysis. In other words, normal cells were found to exhibit lower susceptibility to complement injury. This finding may explain the recent observation that the CC of young eyes remain healthy despite significant MAC deposition.[11] Furthermore, our observation that cells preincubated with lower doses of FBS do not exhibit greater sensitivity to complement attack likely rules out any potential contribution of (FBS starvation-induced) autophagy in complement-mediated cell lysis seen in our assays.

To understand how senescent ECs become more susceptible to complement injury, we looked at the potential role of EC stiffness. This is because (1) aging has been associated with stiffening of retinal vessels and the sclera,[12,13] thus raising the possibility that choroidal ECs/vessels also become stiffer with aging/senescence; (2) nonophthalmic vessels such as aorta and arteries that become stiffer with age[32,33] also exhibit greater

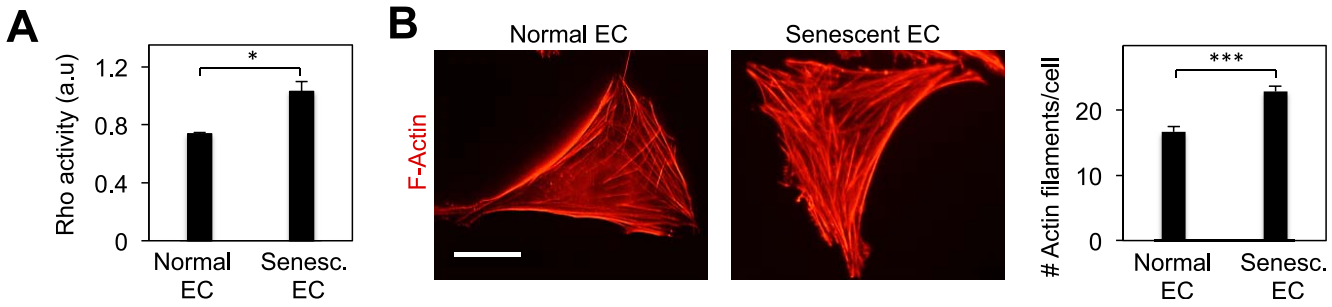

Figure 4. Rho activity is higher in senescent ECs. **(A)** Baseline RhoA activity in normal and senescent RF/6A ECs was measured using RhoA G-LISA activation assay. Absorbance measurements show a ~40% increase in Rho activity in senescent RF/6A ECs when compared with normal cells. * $P < 0.05$. *Bars* indicate average ± standard error of mean. **(B)** We stained RF/6A ECs with fluorescently labeled phalloidin to visualize actin cytoskeletal filaments. Representative fluorescent images and quantitative analysis of actin filament density (*bar graph*; $n \geq 30$) revealed a 35% increase in actin filament density in senescent cells. *** $P < 0.001$. *Bars* indicate average ± standard error of mean. *Scale bar*: 50 μm.

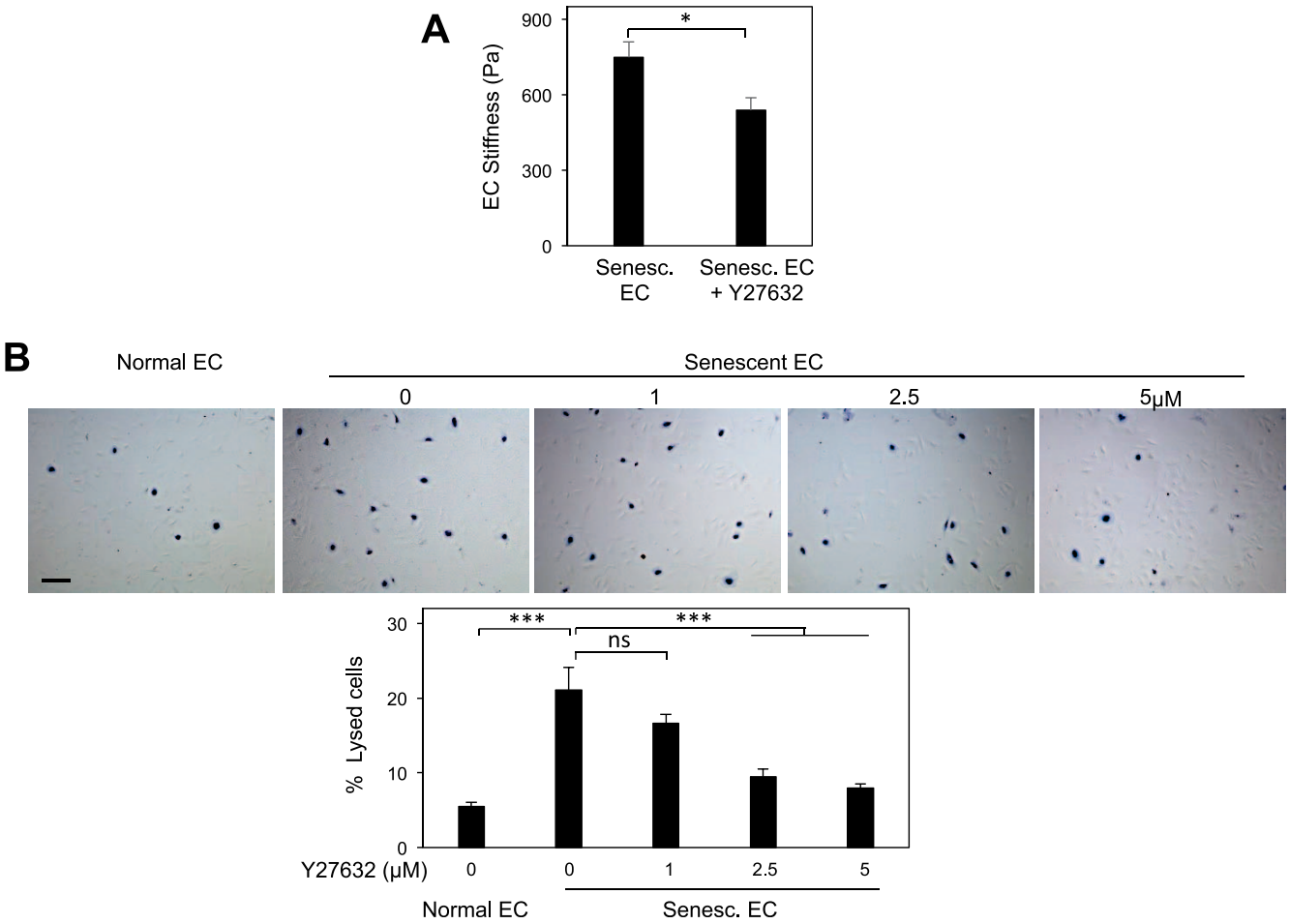

Figure 5. Inhibition of Rho activity prevents MAC-induced lysis of senescent ECs. (**A**) Stiffness of ECs was measured by AFM. Quantitative analysis of multiple ($n \geq 30$) force indentation measurements revealed a ~30% decrease in the stiffness of senescent ECs treated with Y27632 (5 μM), a pharmacological Rho/ROCK inhibitor. * $P < 0.05$. *Bars* indicate average ± standard error of mean. (**B**) Senescent RF/6A ECs were cotreated with NHS and different doses of Y27632 prior to addition of trypan blue. Representative brightfield images and counting of trypan blue-loaded cells (*bar graph*; $n \geq 200$ cells) indicate a progressive decrease in complement-induced lysis of senescent cells with increasing dose of Y27632. *** $P < 0.001$. *Bars* indicate average ± standard error of mean. *Scale bar*: 100 μm.

sensitivity to proinflammatory cues such as low density lipoporotein[14,16]; and (3) senescence has recently been shown to correlate with increased cytoskeletal tension (a measure of stiffness) in umbilical vein-derived ECs.[49] To determine whether senescence leads to choroidal EC stiffening, we performed force indentation measurements using a biological-grade AFM. Atomic force microscope offers a precise, reliable, and analytical technique that we and others have used widely to determine the stiffness of soft biological samples including living cells, extracellular matrices, and soft tissues.[22,50–52] These AFM measurements confirmed our hypothesis that senescent choroidal ECs are significantly stiffer than their normal counterparts.

Mechanistically, cell stiffness is regulated by Rho that, via its downstream target ROCK (Rho-associated Kinase), modulates both actin/myosin-based cytoskeletal tension (contractility) and cortical actin network formation.[19,34] Specifically, past studies by us and others have shown that stiffer, more contractile ECs with dense actin cytoskeletal filaments exhibit high Rho/ROCK activity while inhibition of Rho/ROCK suppresses these effects.[17,20] Consistent with these findings, we here show that the stiffer senescent choroidal ECs exhibit significantly higher Rho activity, which correlates strongly with a concomitant increase in actin microfilament density. That treatment of senescent ECs with ROCK inhibitor Y27632 significantly inhibited cell stiffness confirms the role of Rho in senescent choroidal EC stiffening.

Importantly, we show that this Rho/ROCK-dependent stiffening of senescent choroidal ECs contributes actively to their increased susceptibility to complement injury because pharmacological inhibition of Rho/ROCK significantly inhibited MAC-induced lysis of these cells. Although these findings are the first to implicate Rho-associated cell stiffness in complement injury, they are generally consistent with the proinflammatory effects of increased Rho/ROCK activity and EC stiffness.[34] Furthermore, if increased cell stiffness indeed plays an important causative role in MAC susceptibility, then increasing the stiffness of normal ECs should increase their MAC-induced lysis. Indeed, we found that pharmacologic activation of Rho/ROCK in normal ECs alone leads to a significant increase in complement injury.

To our knowledge, the current findings are the first to implicate a specific age/senescence-related factor (i.e., Rho-mediated choroidal EC stiffening) in CC atrophy associated with dry AMD.[6] To determine their translational potential, however, these new findings will need to be validated in

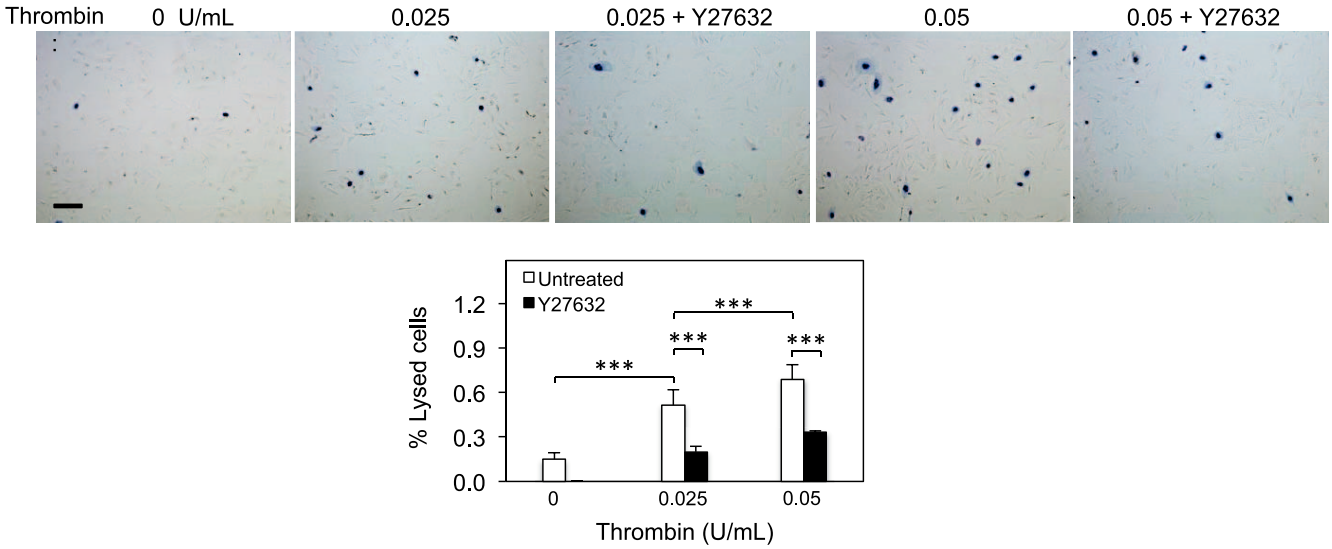

Figure 6. Increasing Rho-mediated tension promotes complement-induced EC lysis. Normal RF/6A ECs were cotreated with NHS and different doses of thrombin, a Rho agonist, prior to addition of trypan blue. Representative images and counting of trypan blue–loaded cells (*bar graph*; $n \geq 150$ cells) indicate a progressive increase in complement-induced lysis of normal RF/6A ECs with increasing thrombin dose. However, cotreatment of thrombin with pharmacologic Rho/ROCK inhibitor Y27632 (5 μM) significantly prevented cell lysis. *** $P < 0.001$. *Bars* indicate average ± standard deviation. *Scale bar*: 100 μm.

appropriate animal models of dry AMD, such as the rhesus macaque monkeys that share the same AMD susceptibility genes *ARMS2* and *HTRA1* with humans, and undergo drusen accumulation as seen in humans.[53,54] Further, although our findings offer new mechanistic insight into choroidal EC loss and CC degeneration associated with dry AMD, they do not yet explain precisely how cell stiffness increases EC sensitivity to complement injury. In this regard, it must be noted that host tissue cells protect themselves from incessant MAC attack, resulting from the continuously activated alternative complement pathway, by expressing surface inhibitors of MAC pore formation.[55,56] Intriguingly, we show that both normal and senescent ECs express similar levels of surface CD59, an endogenous membrane-bound regulator of the complement system that specifically blocks the assembly and formation of transmembrane MAC pores ($C5b\text{-}9_n$) by interacting with the terminal complement proteins C8 and C9, thus preventing C9 polymerization. Given the similarity in CD59 "expression" levels, it is possible that the greater sensitivity of senescent ECs to complement attack results from Rho (tension)-mediated alteration in CD59 conformation, and thereby its "activity"; however, this remains to be carefully examined in a separate study.

Additionally, AMD is a multifactorial disease that is also regulated by dietary and genetic factors.[53,54,57,58] How these risk factors contribute to the age-related mechanical control of CC susceptibility to complement injury also remains to be determined. A detailed examination of the molecular pathways underlying this mechanical control of choroidal EC dysfunction may lead to the identification of new therapeutic targets for CC atrophy and AMD progression.

Acknowledgments

The authors thank Ronald Gorham Jr, Nehemiah Zewde, Dimitrios Morikis (UCR; Bioengineering) for helpful discussions regarding studies involving complement activation and Patrick Shelar (UCR, CMDB Program) for help with preliminary EC senescence studies.

Supported by Initial Complement Funds provided by the UC Riverside Bourns College of Engineering.

Disclosure: **A.P. Cabrera**, None; **A. Bhaskaran**, None; **J. Xu**, None; **X. Yang**, None; **H.A. Scott**, None; **U. Mohideen**, None; **K. Ghosh**, None

References

1. Cook HL, Patel PJ, Tufail A. Age-related macular degeneration: diagnosis and management. *Br Med Bull*. 2008;85:127–149.
2. Friedman DS, O'Colmain BJ, Munoz B, et al. Prevalence of age-related macular degeneration in the United States. *Arch Ophthalmol*. 2004;122:564–572.
3. Ambati J, Fowler BJ. Mechanisms of age-related macular degeneration. *Neuron*. 2012;75:26–39.
4. Zhang K, Zhang L, Weinreb RN. Ophthalmic drug discovery: novel targets and mechanisms for retinal diseases and glaucoma. *Nat Rev Drug Discov*. 2012;11:541–559.
5. Whitmore SS, Sohn EH, Chirco KR, et al. Complement activation and choriocapillaris loss in early AMD: implications for pathophysiology and therapy. *Prog Retin Eye Res*. 2015;45:1–29.
6. Mullins RF, Johnson MN, Faidley EA, Skeie JM, Huang J. Choriocapillaris vascular dropout related to density of drusen in human eyes with early age-related macular degeneration. *Invest Ophthalmol Vis Sci*. 2011;52:1606–1612.
7. McLeod DS, Grebe R, Bhutto I, Merges C, Baba T, Lutty GA. Relationship between RPE and choriocapillaris in age-related macular degeneration. *Invest Ophthalmol Vis Sci*. 2009;50:4982–4991.
8. McLeod DS, Taomoto M, Otsuji T, Green WR, Sunness JS, Lutty GA. Quantifying changes in RPE and choroidal vasculature in eyes with age-related macular degeneration. *Invest Ophthalmol Vis Sci*. 2002;43:1986–1993.
9. Parmeggiani F, Romano MR, Costagliola C, et al. Mechanism of inflammation in age-related macular degeneration. *Mediators Inflamm*. 2012;2012:546786.

10. Anderson DH, Mullins RF, Hageman GS, Johnson LV. A role for local inflammation in the formation of drusen in the aging eye. *Am J Ophthalmol*. 2002;134:411–431.
11. Mullins RF, Schoo DP, Sohn EH, et al. The membrane attack complex in aging human choriocapillaris: relationship to macular degeneration and choroidal thinning. *Am J Pathol*. 2014;184:3142–3153.
12. Friedman E, Ivry M, Ebert E, Glynn R, Gragoudas E, Seddon J. Increased scleral rigidity and age-related macular degeneration. *Ophthalmology*. 1989;96:104–108.
13. Kotliar KE, Baumann M, Vilser W, Lanzl IM. Pulse wave velocity in retinal arteries of healthy volunteers. *Br J Ophthalmol*. 2011;95:675–679.
14. Wang M, Monticone RE, Lakatta EG. Proinflammation of aging central arteries: a mini-review. *Gerontology*. 2014;60:519–529.
15. Laurent S. Defining vascular aging and cardiovascular risk. *J Hypertens*. 2012;(suppl 30):S3–S8.
16. Kothapalli D, Liu SL, Bae YH, et al. Cardiovascular protection by ApoE and ApoE-HDL linked to suppression of ECM gene expression and arterial stiffening. *Cell Rep*. 2012;2:1259–1271.
17. Ghosh K, Thodeti CK, Dudley AC, Mammoto A, Klagsbrun M, Ingber DE. Tumor-derived endothelial cells exhibit aberrant Rho-mediated mechanosensing and abnormal angiogenesis in vitro. *Proc Natl Acad Sci U S A*. 2008;105:11305–11310.
18. Mammoto A, Mammoto T, Kanapathipillai M, et al. Control of lung vascular permeability and endotoxin-induced pulmonary oedema by changes in extracellular matrix mechanics. *Nat Commun*. 2013;4:1759.
19. Mammoto A, Mammoto T, Ingber DE. Rho signaling and mechanical control of vascular development. *Curr Opin Hematol*. 2008;15:228–234.
20. Huynh J, Nishimura N, Rana K, et al. Age-related intimal stiffening enhances endothelial permeability and leukocyte transmigration. *Sci Transl Med*. 2011;3:112ra122.
21. Yang X, Scott HA, Ardekani S, Williams M, Talbot P, Ghosh K. Aberrant cell and basement membrane architecture contribute to sidestream smoke-induced choroidal endothelial dysfunction. *Invest Ophthalmol Vis Sci*. 2014;55:3140–3147.
22. Yang X, Scott HA, Monickaraj F, et al. Basement membrane stiffening promotes retinal endothelial activation associated with diabetes. *FASEB J*. 2016;30:601–611.
23. Scott HA, Quach B, Yang X, et al. Matrix stiffness exerts biphasic control over monocyte-endothelial adhesion via Rho-mediated ICAM-1 clustering. *Integr Biol (Camb)*. 2016;8:869–878.
24. Debacq-Chainiaux F, Erusalimsky JD, Campisi J, Toussaint O. Protocols to detect senescence-associated beta-galactosidase (SA-betagal) activity, a biomarker of senescent cells in culture and in vivo. *Nat Protoc*. 2009;4:1798–1806.
25. Campisi J, Robert L. Cell senescence: role in aging and age-related diseases. *Interdiscip Top Gerontol*. 2014;39:45–61.
26. Campisi J. Aging cellular senescence, and cancer. *Annu Rev Physiol*. 2013;75:685–705.
27. Campisi J, d'Adda di Fagagna F. Cellular senescence: when bad things happen to good cells. *Nat Rev Mol Cell Biol*. 2007;8:729–740.
28. Johnson LV, Forest DL, Banna CD, et al. Cell culture model that mimics drusen formation and triggers complement activation associated with age-related macular degeneration. *Proc Natl Acad Sci U S A*. 2011;108:18277–18282.
29. Gorham RD Jr, Forest DL, Tamamis P, et al. Novel compstatin family peptides inhibit complement activation by drusen-like deposits in human retinal pigmented epithelial cell cultures. *Exp Eye Res*. 2013;116:96–108.
30. Chen CS, Mrksich M, Huang S, Whitesides GM, Ingber DE. Geometric control of cell life and death. *Science*. 1997;276:1425–1428.
31. Ghosh K, Ingber DE. Micromechanical control of cell and tissue development: implications for tissue engineering. *Adv Drug Deliv Rev*. 2007;59:1306–1318.
32. Kovacic JC, Moreno P, Nabel EG, Hachinski V, Fuster V. Cellular senescence vascular disease, and aging: part 2 of a 2-part review: clinical vascular disease in the elderly. *Circulation*. 2011;123:1900–1910.
33. Kovacic JC, Moreno P, Hachinski V, Nabel EG, Fuster V. Cellular senescence, vascular disease, and aging: part 1 of a 2-part review. *Circulation*. 2011;123:1650–1660.
34. Huveneers S, Daemen MJ, Hordijk PL. Between Rho(k) and a hard place: the relation between vessel wall stiffness endothelial contractility, and cardiovascular disease. *Circ Res*. 2015;116:895–908.
35. Cuerrier CM, Gagner A, Lebel R, Gobeil F Jr, Grandbois M. Effect of thrombin and bradykinin on endothelial cell mechanical properties monitored through membrane deformation. *J Mol Recognit*. 2009;22:389–396.
36. Birukova AA, Smurova K, Birukov KG, Kaibuchi K, Garcia JG, Verin AD. Role of Rho GTPases in thrombin-induced lung vascular endothelial cells barrier dysfunction. *Microvasc Res*. 2004;67:64–77.
37. Birukova AA, Tian X, Cokic I, Beckham Y, Gardel ML, Birukov KG. Endothelial barrier disruption and recovery is controlled by substrate stiffness. *Microvasc Res*. 2013;87:50–57.
38. Krisinger MJ, Goebeler V, Lu Z, et al. Thrombin generates previously unidentified C5 products that support the terminal complement activation pathway. *Blood*. 2012;120:1717–1725.
39. Sennlaub F, Auvynet C, Calippe B, et al. CCR2(+) monocytes infiltrate atrophic lesions in age-related macular disease and mediate photoreceptor degeneration in experimental subretinal inflammation in Cx3cr1 deficient mice. *EMBO Mol Med*. 2013;5:1775–1793.
40. Skeie JM, Mullins RF. Macrophages in neovascular age-related macular degeneration: friends or foes? *Eye (Lond)*. 2009;23:747–755.
41. Baker DJ, Wijshake T, Tchkonia T, et al. Clearance of p16Ink4a-positive senescent cells delays ageing-associated disorders. *Nature*. 2011;479:232–236.
42. Lou D, Hu F. Co-distribution of von Willebrand factor and fibronectin in cultured rhesus endothelial cells. *Histochem J*. 1987;19:431–438.
43. Ottino P, Finley J, Rojo E, et al. Hypoxia activates matrix metalloproteinase expression and the VEGF system in monkey choroid-retinal endothelial cells: involvement of cytosolic phospholipase A2 activity. *Mol Vis*. 2004;10:341–350.
44. Amrite AC, Kompella UB. Celecoxib inhibits proliferation of retinal pigment epithelial and choroid-retinal endothelial cells by a cyclooxygenase-2-independent mechanism. *J Pharmacol Exp Ther*. 2008;324:749–758.
45. Kim NW, Piatyszek MA, Prowse KR, et al. Specific association of human telomerase activity with immortal cells and cancer. *Science*. 1994;266:2011–2015.
46. Camous L, Roumenina L, Bigot S, et al. Complement alternative pathway acts as a positive feedback amplification of neutrophil activation. *Blood*. 2011;117:1340–1349.
47. Rutar M, Valter K, Natoli R, Provis JM. Synthesis and propagation of complement C3 by microglia/monocytes in the aging retina. *PLoS One*. 2014;9:e93343.
48. Luo C, Zhao J, Madden A, Chen M, Xu H. Complement expression in retinal pigment epithelial cells is modulated by activated macrophages. *Exp Eye Res*. 2013;112:93–101.
49. Cheung TM, Yan JB, Fu JJ, Huang J, Yuan F, Truskey GA. Endothelial cell senescence increases traction forces due to age-associated changes in the glycocalyx and SIRT1. *Cell Mol Bioeng*. 2014;8:63–75.

Investigative Ophthalmology & Visual Science

50. Lehenkari PP, Charras GT, Nykanen A, Horton MA. Adapting atomic force microscopy for cell biology. *Ultramicroscopy*. 2000;82:289–295.
51. Adams WJ, O'Grady ML, Ghosh K, Gibbs AD, Geisse NA, Ingber DE, Parker KK. Viscoelastic indentation of extremely soft biological samples. *Biophysical J*. 2009;96:398a.
52. Ghosh K, Pan Z, Guan E, et al. Cell adaptation to a physiologically relevant ECM mimic with different viscoelastic properties. *Biomaterials*. 2007;28:671–679.
53. Pennesi ME, Neuringer M, Courtney RJ. Animal models of age related macular degeneration. *Mol Aspects Med*. 2012;33:487–509.
54. Francis PJ, Appukuttan B, Simmons E, et al. Rhesus monkeys and humans share common susceptibility genes for age-related macular disease. *Hum Mol Genet*. 2008;17:2673–2680.
55. Acosta J, Hettinga J, Fluckiger R, et al. Molecular basis for a link between complement and the vascular complications of diabetes. *Proc Natl Acad Sci U S A*. 2000;97:5450–5455.
56. Lee MS, Jones T, Song DY, Jang JH, Jung JU, Gao SJ. Exploitation of the complement system by oncogenic Kaposi's sarcoma-associated herpesvirus for cell survival and persistent infection. *PLoS Pathog*. 2014;10:e1004412.
57. Koo E, Neuringer M, SanGiovanni JP. Macular xanthophylls lipoprotein-related genes, and age-related macular degeneration. *Am J Clin Nutr*. 2014;(100 suppl 1):336S–346S.
58. Barker FM II, Snodderly DM, Johnson EJ, et al. Nutritional manipulation of primate retinas, V: effects of lutein, zeaxanthin, and n-3 fatty acids on retinal sensitivity to blue-light-induced damage. *Invest Ophthalmol Vis Sci*. 2011;52:3934–3942.

Investigative Ophthalmology & Visual Science

Supplemental Figure 1

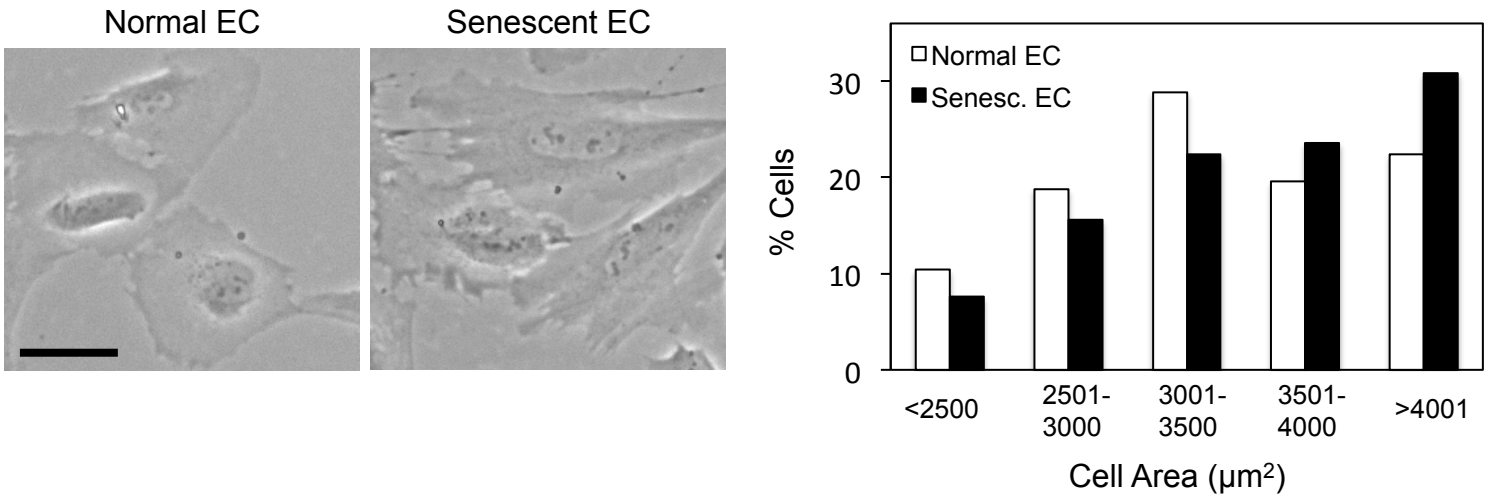

SUPPLEMENTAL FIGURE 1. Senescence leads to an increase in cell area. Representative phase contrast images and measurement of projected cell area (histogram; n=250 cells) together indicate that senescent ECs are markedly larger than their normal counterparts. Scale bar: 50 μm.

Supplemental Figure 2

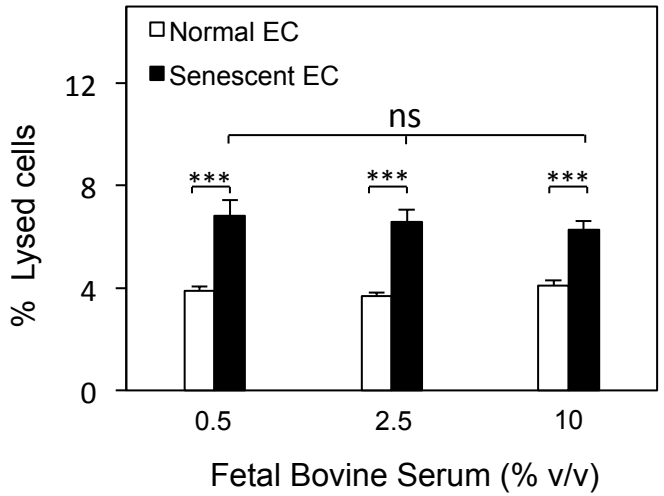

SUPPLEMENTAL FIGURE 2. Effect of FBS pre-incubation on susceptibility to complement injury. RF/6A ECs were plated in medium containing different concentrations of FBS (0.5, 2.5, and 10% v/v) for 6h prior to NHS treatment. Lysis of NHS treated-cells was detected by trypan blue exclusion assay. Counting of trypan blue-loaded cells (bar graph; n≥200 cells) reveals that there is no difference in the degree of lysis between ECs pre-incubated with the three FBS doses (ns, no significance). Bars indicate average ± standard error of mean.

Supplemental Figure 3

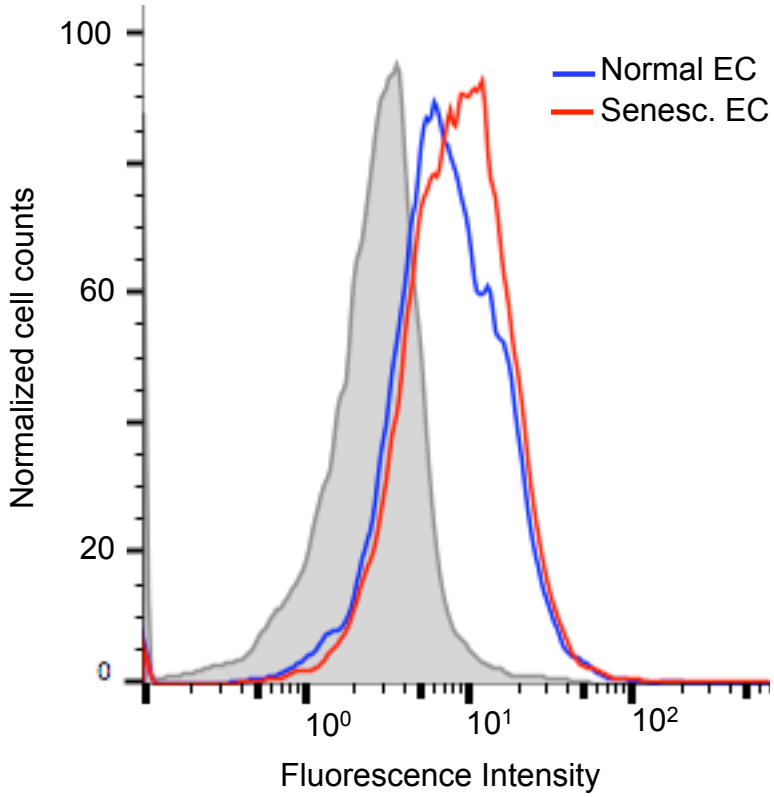

SUPPLEMENTAL FIGURE 3. CD59 expression. Normal and senescent ECs were labeled with anti-CD59 or isotype-matched control antibody (solid gray histogram), and subjected to flow cytometry. Histograms of cell counts vs fluorescence indicate that both normal and senescent cells exhibit similar expression levels of cell surface CD59.